Dalton Transactions

PAPER

View Article Online
View Journal

Cite this: DOI: 10.1039/c5dt01250c

Synthesis of copper ion incorporated horseradish peroxidase-based hybrid nanoflowers for enhanced catalytic activity and stability†

Burcu Somturk,[a] Mehmet Hancer,[b] Ismail Ocsoy*[b,c] and Nalan Özdemir*[a]

Received 31st March 2015,
Accepted 21st April 2015

DOI: 10.1039/c5dt01250c

www.rsc.org/dalton

In this study, we report the preparation, catalytic activity and stability of a hybrid nanoflower (hNF) formed from horseradish peroxidase (HRP) enzyme and copper ions (Cu^{2+}). We studied the morphology of hNFs as a function of the concentrations of copper (Cu^{2+}) ions, chloride ions (Cl^-) and HRP enzyme, the pH of the buffer solution (phosphate buffered saline), and the temperature of the reaction. The effects of morphology on the catalytic activity and stability of hNFs were evaluated by oxidation of guaiacol (2-methoxyphenol) to colored 3,3-dimethoxy-4,4-diphenoquinone in the presence of hydrogen peroxide (H_2O_2). The enhanced activity of hNFs synthesized (from 0.02 mg mL^{-1} HRP in 10 mM PBS (pH 7.4) at +4 °C) was 17 595 U mg^{-1}, which was ~300% higher than free HRP in PBS, where it achieved an activity of 5952 U mg^{-1}. In terms of stability, these hNFs stored in PBS buffer at +4 °C and room temperature (RT = 20 °C) lost 4% and 20%, respectively, of their initial catalytic activities within 30 days. Finally, we demonstrated that these hNFs can be utilized as sensors for the detection of dopamine.

1. Introduction

As natural biocatalysts, enzymes have received considerable attention owing to their unique properties, including high catalytic activity, stability, selectivity, low toxicity and water solubility. Accordingly, they have found widespread use in various scientific and technical fields, including chemistry, biochemistry, medicine, pharmaceutical science and industry (textile, food, *etc.*).[1–5] However, the instability of the free enzymes in aqueous solution strictly limits their applications. To address this issue, two common methods, chemical modification and immobilization, have been used to enhance the enzyme catalytic activity and stability. Although chemically modified enzymes have exhibited high stability, they have not shown a remarkable increase in catalytic activity. Furthermore, the time-consuming and labor-intensive synthetic procedures have limited application of the chemical modification method.[6–8]

In contrast to chemical modification, immobilization of enzymes in/on solid supports has offered a simple, alternative, generally requiring one-step reaction. In general, immobilized enzymes show improved stability, making them efficient, reusable and economical. Over the past two decades, enzymes have been immobilized in/on various supports, such as mesoporous silica, inorganic or organic nanomaterials, polymer strands and sol–gel materials through covalent, non-covalent, entrapment and cross-linking interactions.[9–13] Nanomaterials with their high surface-to-volume ratios serve as platforms capable of loading significantly more enzyme. Immobilization of enzymes generally enhances the stability, presumably due to reduced mobility and attachment of more enzymes per volume unit of the support compared to the free enzyme dissolved in solution.[14–25] However, increased catalytic activity is generally limited due to mass transfer limitations between the enzyme and the substrate and conformational changes in the enzyme.[26–34] Therefore, there is still a high demand for immobilized enzymes with enhanced catalytic activity and stability.

Recently, Zare and co-workers reported an elegant approach for the synthesis of immobilized enzymes in the form of nanoflowers with highly enhanced catalytic activity and stability.[35,36] Zare and co-workers also reported synthesis of a membrane containing laccase nanoflowers for detection of phenol.[37] In subsequent studies, Zeng and co-workers utilized the same synthetic route to produce $CaHPO_4$-α-amylase-based

[a]Department of Chemistry, Faculty of Science, Erciyes University, Kayseri, 38039 Turkey. E-mail: ozdemirn@erciyes.edu.tr
[b]Nanotechnology Research Center (ERNAM), Erciyes University, Kayseri, 38039 Turkey. E-mail: ismailocsoy@erciyes.edu.tr
[c]Department of Analytical Chemistry, Faculty of Pharmacy, Erciyes University, Kayseri, 38039 Turkey

†Electronic supplementary information (ESI) available: SEM images of Cl^- and HRP enzyme concentration dependent hNFs and the SEM image of hNFs after activity measurements; photos of guaiacol in PBS buffer, the mixture of hNFs and guaiacol before activity measurements and the mixture of hNFs and guaiacol stored at RT for 2 months; activities of hNFs synthesized at different pH values. See DOI: 10.1039/c5dt01250c

nanoflowers[38] and Yang and co-workers used enzyme-inorganic nanoflowers as sensors for detection of hydrogen peroxide and phenol.[39] Despite these reports, the underlying principles of nanoflower formation and increased catalytic activity and stability still remain elusive, and further studies are needed to explore effects of reaction parameters on the morphology of nanoflowers and to elucidate the mechanism of enhancement of enzyme activity and stability. Herein, we present a study on the formation, catalytic activity and stability of hybrid nanoflowers (hNFs) containing horseradish peroxidase (HRP) enzyme and copper ions (Cu^{2+}). The main goals were to evaluate the effect of reaction parameters on formation of hNFs and to explain the enhancements in the activity and stability at different storage temperatures. The NFs exhibited dramatically enhanced activity due to these potential reasons: (1) the high surface area of hNFs, which alleviates mass-transfer limitations, (2) cooperative effects due to nanoscale-entrapped HRP, and (3) favorable HRP conformation in hNFs.

2. Experimental

2.1 Chemicals and materials

Copper(II) sulfate pentahydrate ($CuSO_4 \cdot 5H_2O$), albumin from bovine serum (BSA) (lyophilized powder) and peroxidase from horseradish (HRP) (lyophilized powder, beige, ~150 U mg^{-1}, Enzyme Commission (EC) Number 1.11.1.7), guaiacol and dopamine hydrochloride were obtained from Sigma-Aldrich. Salts (NaCl, KCl, Na_2HPO_4, KH_2PO_4, $CaCl_2 \cdot 2H_2O$, $MgCl_2 \cdot 6H_2O$) were also purchased from Sigma-Aldrich. Ultrapure water (18.2 MΩ; Millipore Co., USA) was used in all experiments.

2.2 Synthesis of HRP–Cu^{2+} hybrid nanoflowers

The synthesis of hNFs was accomplished using a modified method.[35] First, a 120 mM $CuSO_4$ stock solution in ultrapure water was freshly prepared. Then, 60 μL of $CuSO_4$ stock solution was added to 9 mL of 10 mM PBS solution (pH 7.4), containing 0.02 mg mL^{-1} HRP. This final mixture was vigorously agitated, and was then left undisturbed for incubation for 72 hours at two different temperatures, +4 °C and room temperature (RT = 20 °C). After incubation, the growth process of hNFs was complete and the mixture was centrifuged to obtain a blue-colored precipitate (indication of hNF formation). The collected hNF powder was washed at least 3 times with water and centrifuged at 12 000 rpm for 20 min in order to remove unreacted components. Finally, the hNF precipitates were dried under vacuum at room temperature.

2.3 Enzyme activity measurement

In all activity and stability measurement experiments, the hNFs (prepared from 0.02 mg mL^{-1} HRP and 0.8 mM Cu^{2+}) and an identical concentration of free HRP were used. The activities of hNFs were determined by colorimetric and spectroscopic methods using guaiacol as a chromogenic substrate.[40] In activity measurements with hNFs and free HRP, a standard protocol (pH 6.8, 0.1 M KH_2PO_4, 25 °C) was applied. First, hNFs and free HRP were dissolved in 1 mL of PBS in two separate reaction tubes and then 1 mL of 22.5 mM hydrogen peroxide (H_2O_2) and 1 mL of 45 mM guaiacol were added to each reaction tube. The final concentrations of H_2O_2 and guaiacol in the tubes were determined as 7.5 mM and 15 mM, respectively. The change in color was visually observed with naked eyes and the changes in absorbance values were also monitored for 3 min at 470 nm at 25 °C using a UV-Vis spectrophotometer.

2.4 Dopamine detection test

Various concentrations of dopamine (DA) (10, 20, 40 and 80 μg mL^{-1}) were dissolved in a 1 mM HCl solution. Standard reaction mixtures containing 1 mL of 22.5 mM H_2O_2 and different volumes of DA (30 μL through 240 μL) were freshly prepared and then the same concentrations of 100 μL hNFs and free HRP were separately added to these mixtures. The final volume of the mixtures was adjusted to 3 mL by the addition of PBS (0.1 M, pH 6.8). The change in color was visually observed and the changes in absorbance values were monitored for 50 min at 297 nm at 25 °C using a UV-Vis spectrophotometer.

3. Results and discussion

Morphology evolution with various reaction parameters and the mechanism underlying enzyme activity and stability in terms of hNF morphology, storage temperature and storage time were systematically studied. It is well known that reaction parameters, including precursor concentrations, reaction temperature and reaction time, can influence the morphology of all types of nanomaterials and their physical and chemical properties. In addition, the precursor concentration ratio has a significant impact on the formation of hybrid nanomaterials by controlling the number of nucleation centers.[41–44] In this report, the hNF formation mechanism is described in terms of several reaction parameters.

We chose HRP for this study, owing to its wide catalytic activity, high sensitivity and substrate specificity. It has been widely used in many applications, including removal of phenols from polluted water, organic synthesis, biosensor design, and clinic and micro-analytical studies.[45–48]

3.1 Preparation and characterization of hybrid nanoflowers

In this synthesis strategy described above, Cu^{2+} ions were rationally and successfully combined with HRP to form flower-like hybrid structures called "hybrid nanoflowers". The proposed mechanism of hNF formation is illustrated in Fig. 1. The hNFs contain three major components: phosphate ions from the PBS solution, Cu^{2+} ions and HRP enzyme. The synthesis of hNFs involves three major successive steps: nucleation, growth process and formation. To generate uniform hNFs, it is first necessary to understand the nucleation step, in which Cu^{2+} ions react with phosphate to create primary copper phosphate complexes. The amine groups in the backbone of

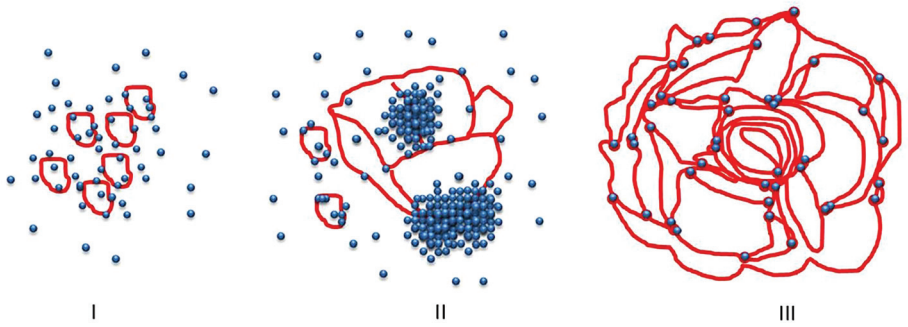

Fig. 1 Possible formation mechanism of HRP–Cu^{2+} hNF divided into three parts: (I) nucleation, (II) growth and (III) completion of the entire hNF formation. Blue dots represent the copper phosphate complex.

HRP preferentially coordinate to copper phosphate to initiate the nucleation of nanocrystals. In the growth process, the primary nanocrystals were continuously fed with HRP to produce large petals on the nanocrystals. The key feature of the growth process is the action of HRP as "glue" to form large assembled branches of HRP (connected to each other), resembling flower petals, on copper phosphate nanocrystals. In the formation, hierarchically and kinetically grown nanocrystals reached the saturation level to complete the growth process. As a consequence, the hNFs were efficiently produced at the end of the anisotropic growth process.

The hNFs were characterized using SEM, EDX analysis, Bradford assay, UV-Vis spectrometry and XRD. The effect of reaction temperatures on the morphology of the hNFs was demonstrated with SEM images (Fig. 2). The hNFs synthesized in PBS (pH 7.4) at +4 °C had spherical shapes with diameters of ~5.5 μm size (Fig. 2A) while the hNFs synthesized at RT gave blooming structures with ~6.5 μm in size. We speculate that the growth process of the hNFs at +4 °C occurred more slowly than that of hNFs at RT. In addition, we assume that HRP molecules bind to copper phosphate nanocrystals more tightly at +4 °C than at RT. In a further study, the effects of HRP and Cu^{2+} concentrations on the formation of the hNFs were determined. When the concentration of HRP was decreased from 0.1 mg mL^{-1} to 0.02 mg mL^{-1}, the hNFs were produced more uniformly and monodisperse (Fig. S1A and S1B in the ESI†). Furthermore, the concentration of Cu^{2+} was also highly important for initiation of the nanocrystals and the growth process. From our results, we determined that the optimal Cu^{2+} concentration was around 0.8 mM to properly form the hNFs. We demonstrated that the Cu^{2+} ion is an indispensable component and a driving force to form primary nanocrystals. For instance, no blue-color precipitates were observed without Cu^{2+} and when the concentration of Cu^{2+} was below 80 μM in PBS because the Cu^{2+} concentrations were not high enough to reach the point of supersaturation needed to initiate nucleation and subsequent growth of copper phosphate nanocrystals. In addition, the Cu^{2+} concentration was

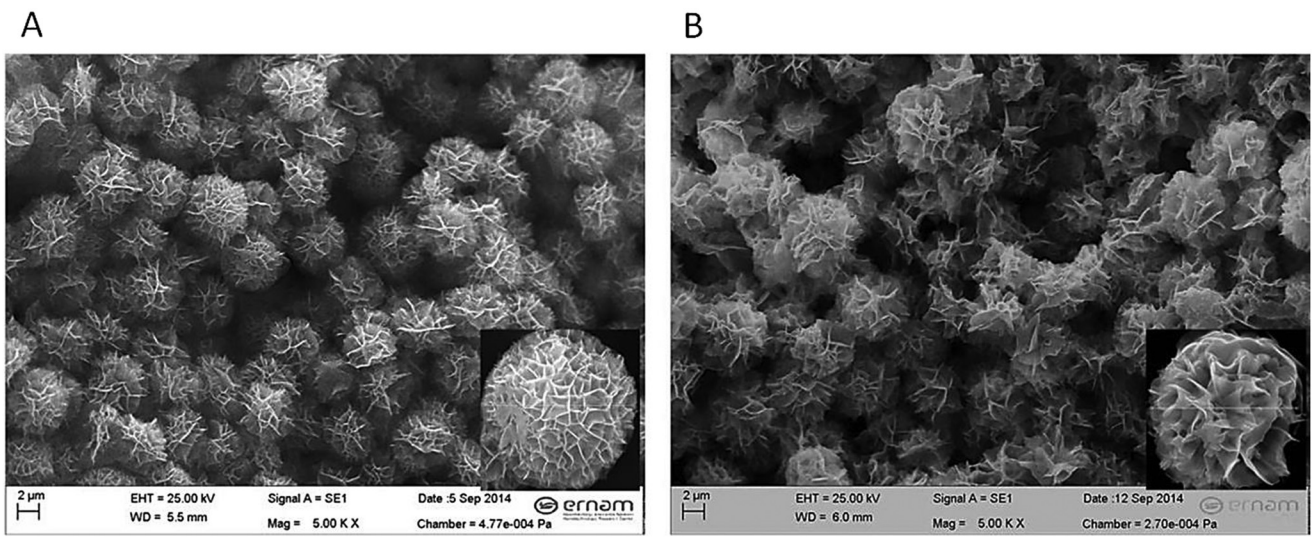

Fig. 2 SEM images of hNFs synthesized at different incubation temperatures (A) +4 °C. Inset: the SEM image of a hNF of (A) with 25.00kx magnification, (B) RT. Inset: the SEM image of a hNF of (B) with 25.00kx magnification.

also a key for determining the number of Cu^{2+} binding sites, which generate separate petals and are fundamental for the formation of the hNFs. In a typical hNF synthesis, HRP and Cu^{2+} were accordingly mixed in a 10 mM PBS solution containing ~140 mM Cl^- to form the hNFs. When the Cl^- concentration was increased 50 fold to ~7 M, the blue-colored precipitates were not observed. We attribute this to the formation of soluble Cu(II) chloride complexes, which prevented the growth of nanocrystals. However, even though blue precipitates were observed at the bottom of the reaction tubes in the absence of Cl^-, no hNFs were formed due to the incomplete growth process, as shown in SEM images in Fig. S1C and S1D in the ESI.†

For further morphology evolution study, the NFs were synthesized at various PBS pH values (pH 6, 8 and 9). The HRP isoelectric point (pI) is 5.5, where free HRP is expected to be neutral, while above and below this value the protein is expected to be negative and positive, respectively. At pH 3, 4 and 5, no blue colored precipitates were observed. Considering that HRP molecules were predominately protonated and positively charged at pH values below the pI, the presence of Cu^{2+} cations and positively charged HRP molecules resulted in very strong repulsions between Cu^{2+} ions and HRP and also among HRP molecules, preventing incorporation of Cu^{2+} and HRP. However, formation of hNFs was achieved at pH 6 through pH 9, as shown in the SEM images presented in Fig. 3.

Spherical hNFs were obtained at pH 6 and 8 (Fig. 3A and B), whereas the shapes were splayed at pH 9 (Fig. 3C) due to repulsion among negatively charged HRP molecules. It is also noteworthy to mention that the hNFs were not able to form at pH 10 and above because of strong negative repulsions, which expel petals of HRP rather than forcing them to bind to each other. Zeta potential measurements were used to determine the charge density and change of charge density on the surfaces of hNFs synthesized at different pH values.[44] The hNFs at pH 6 were negatively charged with −3.89 mV zeta potential due to the slight deprotonation of HRP. When increasing pH values, the hNFs became more negative. The zeta potentials of

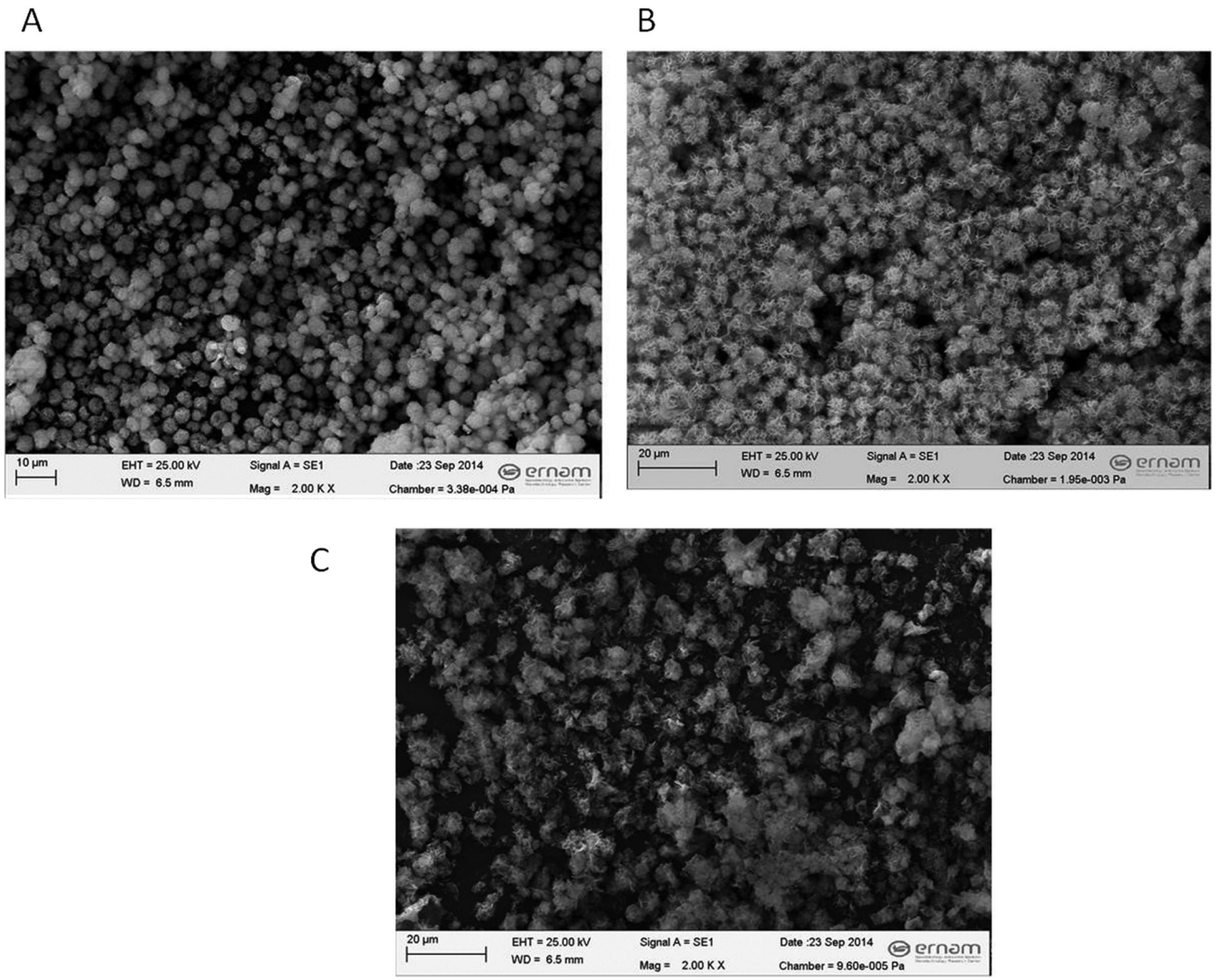

Fig. 3 Formation of the hNFs at different buffer pH values. (A) pH 6, (B) pH 8, and (C) pH 9.

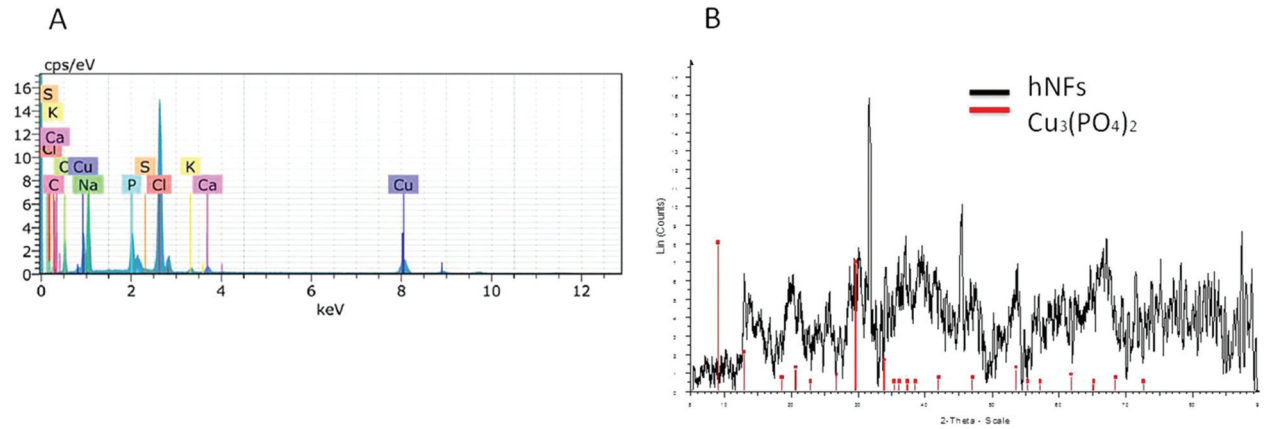

Fig. 4 (A) EDX analysis of the hNFs, (B) XRD patterns of the hNFs (black line). The peak position of the $Cu_3(PO_4)_2{\cdot}3H_2O$ (red line, JCPDS 00-022-0548) located for comparison.

hNFs at pH 7.4, 8, and 9 were −9.35 mV, −14.30 mV and −19.71 mV, respectively. The elemental composition of the hNF powders was analyzed by EDX and peak positions of $Cu_3(PO_4)_2$ in the hNFs were analyzed by XRD. Fig. 4A clearly shows that the weight and atomic percentages of Cu in the hNFs were about 9.3% and 2.8%, respectively. Fig. 4B also reveals that most of the diffraction peaks of $Cu_3(PO_4)_2$ in the hNFs were consistent with those of JCPDS card (00-022-0548). However, we realized that some diffraction peaks may belong to $KCuCl_2$ and $KCuCl_3$ crystals.

3.2 Enzymatic activity and stability measurement of hybrid nanoflowers

The catalytic activities and stabilities were determined using guaiacol as a model substrate for hNFs synthesized under the following experimental conditions: (1) at +4 °C and pH 7.4; (2) RT and pH 7.4; (3) +4 °C and pH 6, 8, and 9. In general, HRP, an oxidoreductase, efficiently catalyzes reactions between the target compound (H-atom donor) and hydrogen peroxide, H_2O_2 (H-atom acceptor). In addition, HRP also catalyzes the oxidation of several organic and inorganic substrates in the presence of H_2O_2.[47–50] In this study, the addition of hNFs to a mixture of guaiacol and H_2O_2 resulted in efficient and rapid oxidation of guaiacol to produce the orange colored quinone type structure, 3,3-dimethoxy-4,4-diphenoquinone (Fig. 5A). This process allowed us to monitor the activity both visually with the naked eye and spectrophotometrically with the increase in the absorbance of the product at 470 nm.

First, hNFs with 98% encapsulation yield (synthesized at +4 °C, pH 7.4) were dissolved in 1 mL of PBS (pH 6.8) and the solution was mixed with guaiacol (45 mM, 1 mL) and H_2O_2 (22.5 mM, 1 mL) in a reaction tube. The resulting mixture was divided into two parts, which were stored at two different temperatures (+4 °C and RT) to determine the influence of storage temperatures (+4 °C and RT) on the catalytic activity and stability of these particular hNFs. Fig. 5B demonstrates that the enhanced activity of hNFs synthesized and stored at +4 °C was 17 595 U mg^{-1}, which was ~300% higher than free HRP in PBS, where it achieved an activity of 5952 U mg^{-1}. However, an activity of 9587 U mg^{-1} was obtained by the use of the hNFs synthesized at RT but stored at +4 °C (data not shown here). In terms of stability, the hNFs stored at +4 °C and RT lost only 4% and 20%, respectively, of their initial activities within 30 days (Fig. 5C). For comparison, Fig. 5C also demonstrates that the same concentration of free HRP stored at +4 °C and RT lost 65% and 92%, respectively, of its initial activity within 30 days. These findings indicate that (1) HRP in the hNFs is much more stable than free HRP in solution; and (2) the storage temperature affects the activity and stability of both hNFs and free HRP. To corroborate the high stability and reusability of these hNFs (synthesized at +4 °C but stored at RT), the nanoflowers used for activity measurements after 30 day storage at RT were stored at RT for two more months. Although these hNFs lost their flower-like shapes and appeared as pressed disc shaped structures (Fig. S2A in the ESI†), they exhibited increased activity compared to HRP in solution but their activity was reduced (~31%) compared to fresh hNFs (data not shown). The color change of guaiacol by the oxidation reaction catalyzed by these pressed disc shaped structures was also observed visually (Fig. S2B(iii) in the ESI†). The mixture of guaiacol and H_2O_2 in PBS is initially colorless before addition of hNFs (Fig. S2B(i) in the ESI†). However, upon addition of fresh hNFs, the color of the mixture changed to intense dark red (Fig. S2B(ii) in the ESI†).

To gain further insight into the impact of reaction temperature on catalysis and stability, both formation and storage of hNFs were carried out at RT (pH 7.4). Fig. 5D shows that these hNFs lost 29.9% of their initial activity within 30 days, whereas the hNFs synthesized at +4 °C showed a lower activity loss (20%), as mentioned above. In addition, the oxidation of guaiacol to colored 3,3-dimethoxy-4,4-diphenoquinone was spectrophotometrically determined at 470 nm, which allows us to quantitatively analyze the activity performance of hNFs and free HRP and to monitor their kinetics. The overall results

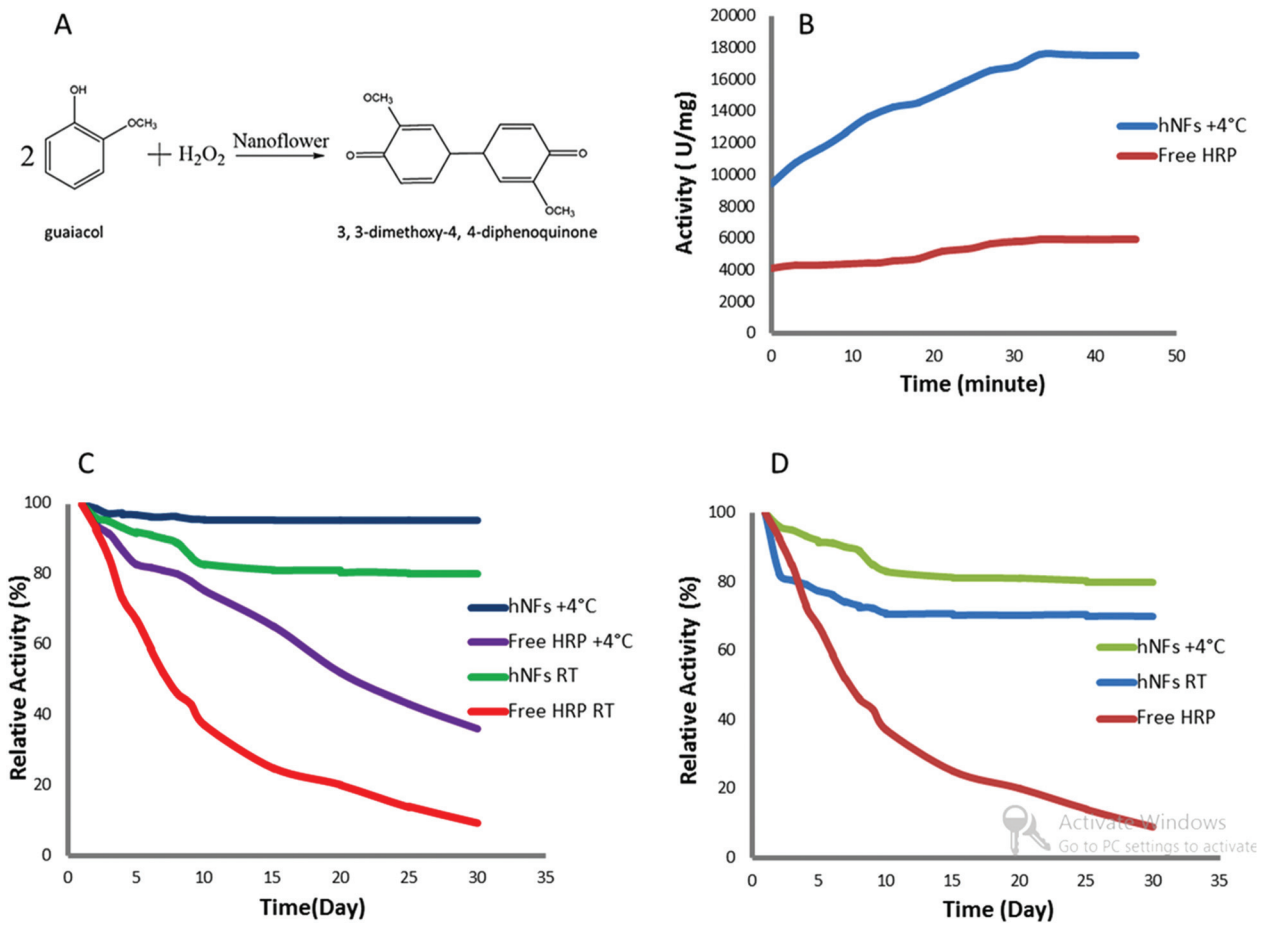

Fig. 5 Activity and stability of nanoflowers and free HRP enzyme towards guaiacol. (A) Formation of the orange quinone type structure "3,3-dimethoxy-4,4-diphenoquinone" from HRP nanoflower catalyzed reaction of guaiacol with H_2O_2. (B) Enhanced activity of nanoflowers synthesized at +4 °C and free HRP measurements. (C) Stability of nanoflowers synthesized at +4 °C measured at +4 °C (blue line) and RT (green line) and free HRP enzyme measured at +4 °C (purple line) and RT (red line.) (D) Stability of nanoflowers synthesized at +4 °C (green line) and RT (blue line) and free HRP enzyme (dark red line) measured at RT.

show that the formation temperatures of hNFs play a role in the activity and stability of hNFs. We suggest that the hNFs should be synthesized and stored at +4 °C to obtain the best activity and stability. The hNFs appeared more compact when prepared at +4 °C and HRP assembled with the favorable conformation in hNFs and both effects may result in decreased mass transfer limitations and induce an enhancement in activity and stability.

Although we proved that hNFs synthesized under particular experimental conditions (at +4 °C and pH 7.4) exhibited dramatically improved activity and stability, a further study was carried out to demonstrate the activity performance of the hNFs, which were prepared at different pH values. As presented in the SEM images above, the hNFs produced at different pH values had different shapes and sizes. We believe that these morphological differences substantially affect activities and stabilities of hNFs. Accordingly, hNFs were synthesized at various pH values at +4 °C (pH 6, 8 and 9) and stored at +4 °C. The hNFs prepared at pH 9 lost 11% of their initial activity, whereas those prepared at pH 8 and pH 6 lost 16.8% and 21.5% of their initial activities, respectively, within 30 days. Among hNFs prepared at different pH values, the hNFs prepared at pH 7.4 showed the best catalytic activity and stability with 4% activity loss within 30 days (previously shown in Fig. 5C) as shown in Fig. S3 in the ESI† for comparison. Their high activity is attributed to the morphology of hNFs with a high surface-to-volume ratio and a suitable HRP conformation.

3.3 Visual and spectrometric detection of dopamine

Dopamine (DA), one of the important catecholamine neurotransmitters, is vital to human life. Controlling its level in the mammalian central nervous system provides proper signal transport in nerve cells. In particular, low levels of DA are associated with several serious neurological diseases, such as schizophrenia, Huntington's disease and Parkinsonism.[44,51] Inspired by the excellent catalytic activity of hNFs, we used them as sensors to detect DA by oxidation. We selected the

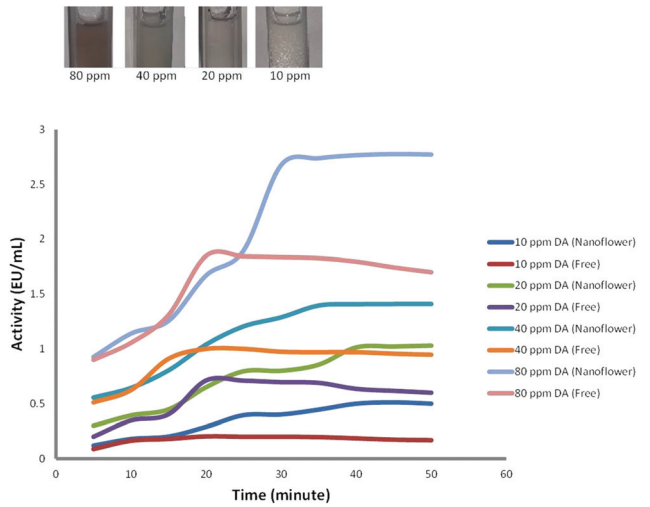

Fig. 6 Kinetics of oxidation of dopamine by HRP nanoflowers and free HRP enzyme. Inset: color changes in dopamine with respective concentrations (10, 20, 40, 80 μg mL^{-1}).

hNFs synthesized at +4 °C in 10 mM PBS (pH 7.4) because of their excellent catalytic activity for the oxidization of DA in the presence of H_2O_2 to an orange colored quinone-type product. The oxidation of DA was visually and spectrometrically detected as shown in Fig. 6. The hNFs catalyzed highly rapid and efficient DA oxidation compared to free HRP. In the standard oxidation procedure, a specified amount of the hNFs was mixed with a series of DA concentrations (10, 20, 40, 80 μg mL^{-1}) in 10 mM PBS buffer (pH 6.8) and absorbance changes were monitored by UV-Vis spectrometry at 485 nm, as well as by visual observation. The color intensified as the concentration of DA was increased. In addition, as the concentration of DA was raised from 10 μg mL^{-1} to 80 μg mL^{-1}, the hNF activity also increased. As a result, the oxidative activities of the hNFs were much higher than that of free HRP at all DA concentrations. It is known that K_M (Michaelis constant) is an important characteristic feature for an enzyme and it shows the affinity of the enzyme to the substrate and the robustness of the enzyme–substrate complex. For this reason, the K_M values of free HRP and hNFs were determined as 0.059 and 0.031 mM, respectively *via* a plot of $1/V$ *versus* $1/[S]$ by the method of Lineweaver and Burk towards dopamine. The lowest K_M of the hNFs dictates that they have enough specificity and efficiency to react with dopamine compared to free HRP.

4. Conclusion

In conclusion, we have investigated the effects of reaction parameters on the morphology, catalytic activity and stability of hNFs composed of Cu^{2+} ions and HRP enzyme. We experimentally explained the impacts of the concentrations of Cu^{2+} ions, Cl^- ions and HRP enzyme, the pH values of PBS, and the reaction temperature on the formation of hNFs. The catalytic activities and stability of a series of hNFs synthesized under different conditions were evaluated, and the results showed that the hNFs exhibited dramatically enhanced activity and stability compared to those of free HRP. We determined that the hNFs obtained from 0.02 mg mL^{-1} HRP in a PBS solution (at +4 °C and pH 7.4) exhibited the best activity and stability within 30 days of storage at +4 °C using guaiacol as a model substrate in the presence of H_2O_2. Furthermore, the hNFs were also successfully applied as sensors for visual and spectrometric detection of the oxidation of dopamine in the presence of H_2O_2 to produce an orange colored quinone-type product.

Author contribution

B.S. performed experiments. I.O. and N.Ö. conceived the original idea and I.O. and N.Ö. supervised the project. I.O., N.Ö. and M.H. designed the project. All authors contributed to the manuscript writing.

Conflict of interest

The authors declare no financial interest.

Acknowledgements

We thank Menekşe Sarihan at the Erciyes University Nanotechnology Research Center for assistance with SEM and EDX measurements. We also appreciate Fatma Kilic Dokan at the Erciyes University Technology Research and Implementation Center for assistance with XRD measurements. This work was supported by a grant from the Erciyes University Scientific Research Office (FBG-2014-5376)2014-2016. We appreciate the comments on the manuscript by Dr Basri Gulbakan as well as the suggestions of Colonel Savas Karatepe.

References

1 J. Kim, J. W. Grate and P. Wang, *Trends Biotechnol.*, 2008, **26**, 639–646.
2 J. Ge, D. Lu, Z. Liu and Z. Liu, *Biochem. Eng. J.*, 2009, **44**, 53–59.
3 P. Wang, *Curr. Opin. Biotechnol.*, 2006, **17**, 574–579.
4 B. Krajewska, *Enzyme Microb. Technol.*, 2004, **35**, 126–139.
5 R. Mesing, *Immobilized Enzymes for Industrial Reactors*, Academic Press, 1995.
6 K. Matsumoto, B. G. Davis and J. B. Jones, *Chem. – Eur. J.*, 2002, **8**, 4129–4137.
7 B. G. Davis, X. Shang, G. DeSantis, R. R. Bott and J. B. Jones, *Bioorg. Med. Chem.*, 1999, **7**, 2293–2301.
8 H. Gron, L. M. Bech, S. Branner and K. Breddam, *Eur. J. Biochem.*, 1990, **194**, 897–901.

9 C. Mateo, J. M. Palomo, G. Fernandez-Lorente, J. M. Guisan and R. Fernandez-Lafuente, *Enzyme Microb. Technol.*, 2007, **40**, 1451–1463.
10 S. Rana, Y. Yeh and V. M. Rotello, *Curr. Opin. Chem. Biol.*, 2010, **14**, 828–834.
11 P. Wang, *Appl. Biochem. Biotechnol.*, 2009, **152**, 343–352.
12 R. A. Sheldon, *Adv. Synth. Catal.*, 2007, **349**, 1289–1307.
13 R. Fernandez-Lafuente, *Enzyme Microb. Technol.*, 2009, **45**, 405–418.
14 J. Kim, J. Park and H. Kim, *Colloids Surf., A*, 2004, **241**, 113–117.
15 J. Lee, J. Kim, J. Kim, H. Jia, M. Kim, J. Kwak, S. Jin, A. Dohnalkova, H. Gyu Park, H. Chang, P. Wang, J. W. Grate and T. Hyeon, *Small*, 2005, **1**, 744–753.
16 D. Avnir, S. Braun, O. Lev and M. Ottolenghi, *Chem. Mater.*, 1994, **6**, 1605–1614.
17 M. T. Reetz, *Adv. Mater.*, 1997, 943–954.
18 I. Gill, *Chem. Mater.*, 2001, **13**, 3404–3421.
19 H. R. Luckarift, J. C. Spain, R. R. Naik and M. O. Stone, *Nat. Biotechnol.*, 2004, **22**, 211–213.
20 A. J. Patil, E. Muthusamy and S. Mann, *Angew. Chem., Int. Ed.*, 2004, **43**, 4928–4949.
21 D. Häring and P. Schreier, *Curr. Opin. Chem. Biol.*, 1999, **3**, 35–38.
22 E. Katz and I. Willner, *Angew. Chem., Int. Ed.*, 2004, **43**, 6042–6108.
23 S. S. Narayanan, R. Sarkar and S. K. Pal, *J. Phys. Chem. C*, 2007, **111**, 11539–11543.
24 T. Shimoboji, E. Larenas, T. Fowler, S. Kulkarni, A. S. Hoffman and P. S. Stayton, *Proc. Natl. Acad. Sci. U. S. A.*, 2002, **99**, 16592–16596.
25 Y. Ito, H. Fujii and Y. Iimanishi, *Biotechnol. Prog.*, 1994, **10**, 398–402.
26 C. W. Wu, J. G. Lee and W. C. Lee, *Biotechnol. Appl. Biochem.*, 1998, **27**, 225–230.
27 J. Oh and J. Kim, *Enzyme Microb. Technol.*, 2000, **27**, 356–361.
28 C. Lee, H. Chiang, K. Li, F. Ko, C. Su and Y. Yang, *Anal. Chem.*, 2009, **81**, 2737–2744.
29 A. Kheirolomoom, F. Khorasheh and H. Fazelinia, *J. Biosci. Bioeng.*, 2002, **93**, 125–129.
30 M. Arica, N. Alaeddinoglu and V. Hasirci, *Enzyme Microb. Technol.*, 1998, **22**, 152–157.
31 T. Godjevargova and K. Gabrovska, *Enzyme Microb. Technol.*, 2006, **38**, 338–342.
32 A. Illanes, J. M. Gonzalez, J. M. Gomez, P. Valencia and L. Wilson, *EJB*, 2010, **13**, 12.
33 C. G. C. Netto, H. E. Toma and L. H. Andrade, *J. Mol. Catal. B: Enzym.*, 2013, **85–86**, 71–92.
34 J. Kim, J. W. Grate and P. Wang, *Chem. Eng. Sci.*, 2006, **61**, 1017–1026.
35 J. Ge, J. Lei and R. N. Zare, *Nature Nanotechnol.*, 2012, **7**, 428–432.
36 L. Zhu, L. Gong, Y. Zhang, R. Wang, J. Ge, Z. Liu and R. N. Zare, *Chem. – Asian J.*, 2013, **8**, 2358–2360.
37 R. Wang, Y. Zhang, D. Lu, J. Ge, Z. Liu and R. N. Zare, *WIREs Nanomed. Nanobiotechnol.*, 2013, **5**, 320–328.
38 L. Wang, Y. Wang, R. He, A. Zhuang, X. Wang, J. Zeng and J. G. Hou, *J. Am. Chem. Soc.*, 2013, **135**, 1272–1275.
39 Z. Lin, Y. Xiao, Y. Yin, W. Hu, W. Liu and H. Yang, *ACS Appl. Mater. Interfaces*, 2014, **6**, 10775–10782.
40 N. C. Veitch, *Phytochemistry*, 2004, **65**, 249–259.
41 I. Ocsoy, B. Gulbakan, M. Shukoor, X. Xiong, T. Chen, D. H. Powell and W. Tan, *ACS Nano*, 2013, **7**, 417–427.
42 X. Ma, Y. Zhao and X. Liang, *Acc. Chem. Res.*, 2011, **44**, 1114–1122.
43 I. Ocsoy, M. L. Paret, M. Arslan Ocsoy, S. Kunwar, T. Chen, M. You and W. Tan, *ACS Nano*, 2013, **7**, 8972–8980.
44 I. Ocsoy, B. Gulbakan, T. Chen, G. Zhu, Z. Chen, M. M. Sari, L. Peng, X. Xiong, X. Fang and W. Tan, *Adv. Mater.*, 2013, **25**, 2319–2325.
45 B. Somtürk, R. Kalın and N. Özdemir, *Appl. Biochem. Biotechnol.*, 2014, **173**, 1815–1828.
46 C. Jun, M. Y. Shao and Z. Peng, *Water Res.*, 2006, **40**, 283–290.
47 T. S. ShaffIqu, J. J. Roy, R. A. Nair and T. E. Abraham, *Appl. Biochem. Biotechnol.*, 2002, **102–103**, 315–326.
48 R. Kalın, A. Atasever and H. Özdemir, *Food Chem.*, 2014, **150**, 335–340.
49 H. Mohsina and R. Khalil-ur, *Food Chem.*, 2009, **115**, 1177–1186.
50 R. Baron, M. Zayats and I. Willner, *Anal. Chem.*, 2005, **77**, 1566–1571.
51 N. Özdemir, A. Çakır and B. Somtürk, *Colloids Surf., A*, 2014, **445**, 40–47.

